

## Electronic instability in inverse- $K_2NiF_4$ -structure $Na_2Sb_2Ti_2O$

W. E. Pickett

*Department of Physics, University of California–Davis, Davis, California 95616*

(Received 4 February 1998)

The layered pnictide titanates  $Na_2Pn_2Ti_2O$ ,  $Pn=Sb$  and  $As$ , display anomalies in the susceptibility and resistivity that have not yet been associated with either magnetic ordering or with structural distortion. Based on local spin-density approximation calculations on the  $Pn=Sb$  member, we find that the nominal ionic picture ( $Na^{+1}$ ,  $Sb^{-3}$ ,  $Ti^{+3} d^1$ ,  $O^{-2}$ ) is reasonably well respected. However, the most likely explanation for the anomaly is not a magnetic transition associated with a local moment on the (nominally)  $Ti^{+3} d^1$  ion. Strong mixing of the Ti  $d$  states with Sb  $p$  and O  $p$  states, as well as direct  $d-d$  overlap, leads to metallic character that delocalizes the Ti  $d$  states. A square “box” Fermi surface that is nearly dispersionless perpendicular to the  $Ti_2O$  layers leads to strong nesting that points to a charge- or spin-density wave instability. We do not obtain any ordered magnetic solutions (having tried ferromagnetic and two types of antiferromagnetic states), which is nominally consistent with a lack of observed magnetic order. [S0163-1829(98)11431-5]

### I. INTRODUCTION

The behavior of spin  $S=\frac{1}{2}$  systems in one (1D) and two (2D) dimensions is currently undergoing intense scrutiny. Whereas the systematics of 1D chains and ladders are beginning to fall into place,<sup>1</sup> the behavior in 2D is less clear. The  $CaV_nO_{2n+1}$  system,  $n=2, 3$ , and 4, comprised of  $1/(n+1)$ -depleted square lattices of  $V^{+4}$  ions, is very instructive; the  $n=3$  member orders (peculiarly), and the  $n=4$  member clearly shows spin gap characteristics, whereas the quasi-1D  $n=2$  member is apparently a spin-Peierls system. Quantum spin liquid behavior has been thought to be at the root of unusual temperature dependences of the magnetic susceptibility at least since O’Keefe and Stone<sup>2</sup> suggested dynamic  $Cu^{+2}$  spin singlet pairing to occur in the high-temperature regime in triclinic  $CuO$ . The 2D triangular lattice compounds  $NaTiO_2$  and  $LiNiO_2$  have been thought to have the frustrated  $S=\frac{1}{2}$  structure speculated by Anderson<sup>3</sup> to have a spin liquid ground state.  $NaTiO_2$ , however, shows evidence of a phase transition around 260 K.<sup>4</sup> Due to such peculiarities, new 2D  $S=\frac{1}{2}$  systems are under great scrutiny.

The very recently studied layered compounds  $Na_2Pn_2Ti_2O$ , with pnictide  $Pn=Sb$  and  $As$ ,<sup>5,6</sup> add a possible new vantage point for studying quantum spin behavior in low dimensions. For  $Pn=Sb$ , the measured susceptibility  $\chi(T)$  shows a sharp drop at  $T^*=114$  K with an accompanying sharp feature in the resistivity  $\rho$ , indicative of some change of phase; the  $Pn=As$  counterpart shows a related but less abrupt drop in  $\chi(T)$  around 250 K. This abrupt drop in  $\chi$  could be due to some change in the spin behavior of the  $Ti^{+3}$  moments.<sup>6</sup> Neither magnetic ordering nor structural change, which could indicate spin-Peierls behavior, at  $T^*$  has yet been observed, but small changes of phase may not have been detected. The  $T$  dependence of  $\chi$  and  $\rho$  is reminiscent of the spin-Peierls compound  $CuGeO_3$ , but the structure is tetragonal—hence at least 2D—whereas  $CuGeO_3$  is of the 1D type of system that is beginning to become understood.

The crystal structure of  $Na_2Sb_2Ti_2O$  (Ref. 5) (we focus on

the  $Pn=Sb$  compound) is the inverse- $K_2NiF_4$ -type shown in Fig. 1. The space group  $I4/mmm$ , and indeed the crystal structure, is identical to that of the (undistorted tetragonal)  $La_2CuO_4$  2D  $S=\frac{1}{2}$  insulator, except that cation sites are occupied by anions, and vice versa. In particular, the transition-metal ion and oxygen ion sites are inverted:  $(La^{+3}O^{-2})_2Cu^{2+}O_2^{-2}$  translates to  $(Sb^{-3}Na^{+1})_2O^{-2}Ti_2^{+3}$ . As a result, O is fourfold coordinated with Ti ions in the layer and twofold coordinated by Na ions along the  $\hat{z}$  axis. Ti is twofold coordinated with O ions in the plane, forming Ti-O chains along both  $\hat{a}$  and  $\hat{b}$  axes that intersect at the O ions. The Ti ion is also fourfold coordinated with Sb ions, forming what can be called  $TiSb_2$  ribbons<sup>6</sup> in analogy with  $CuO_2$  ribbons in  $CuGeO_3$ .

Above  $T^*$ ,  $\chi$  decreases slowly with temperature. The behavior is not fit well by disordered local moment behavior, and might instead be indicative of temperature-dependent

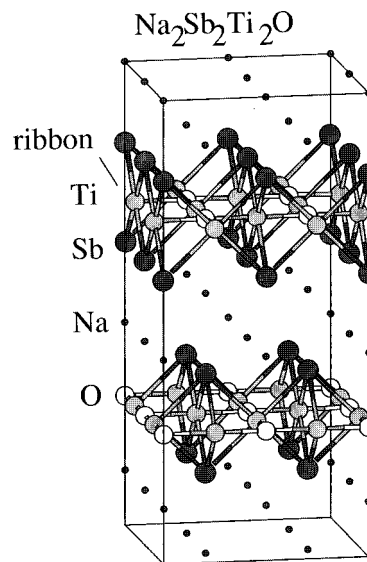


FIG. 1. Layered structure of  $Na_2Sb_2Ti_2O$ ; the figure contains  $2 \times 2 \times 2$  unit cells. A  $TiSb_2$  “ribbon” is noted. Sb is dark gray; Ti is light gray; O is white; Na is the tiny sphere.

renormalization by electron-electron interaction. If the Ti ions are magnetic, it is natural to consider first the intervening O ions as the conduit for possible exchange coupling between Ti ions. However, as they are surrounded by four highly charged ( $\text{Ti}^{+3}$ ) ions, the Madelung potential will lower the O  $p$  state energy with respect to that in common transition-metal oxides, they will become less polarizable, and the superexchange coupling will decrease. The role of coupling through Sb  $p$  states should dominate, since the Sb  $p$  site energy  $\varepsilon_p$  is likely to be nearer the site energy  $\varepsilon_d$  of the Ti ion and the Ti  $d$  orbitals overlap with the Ti  $d$  orbitals, and mixing will be large.

In this paper we confront the electronic and magnetic behavior of this compound. We explore possible magnetic ordering, which would reveal whether exchange interactions are primarily ferromagnetic (FM) or antiferromagnetic (AFM). As is well known,<sup>7-9</sup> knowledge of the character of the occupied orbital(s) of the magnetic ion is fundamental to any understanding of exchange coupling. Another reason for undertaking this study is to extend our inquiry of the treatment by density-functional theory, and specifically the local spin density approximation (LSDA), of  $S = \frac{1}{2}$  ions. In itinerant ferromagnetic (FM) systems LSDA has a very positive record. The description of antiferromagnetism (AFM) especially in small spin systems is less illustrious. The inability to obtain any moment on the  $\text{Cu}^{+2} d^9$  ion in the insulating AFM phases of the layered copper oxides (such as  $\text{La}_2\text{CuO}_4$ ) is the most glaring problem.<sup>10</sup> Treatment of the charge conjugate  $d^1$  ion was more successful in  $\text{CaV}_4\text{O}_9$  ( $\text{V}^{4+}$ ),<sup>9</sup> and the (formally)  $\text{Ti}^{3+}$  ion in this compound is another member of this class.

## II. METHOD OF CALCULATION

We have applied the full potential linearized augmented plane wave (FLAPW) method<sup>11,12</sup> used in many previous studies of magnetic transition metal oxide compounds. The FLAPW sphere radii were chosen to be  $R_{\text{Na}} = 2.70$  a.u.,  $R_{\text{Sb}} = 3.10$  a.u.,  $R_{\text{Ti}} = 2.15$ ,  $R_{\text{O}} = 1.75$  a.u. The semicore states treated with additional local orbitals<sup>12</sup> were Na  $2p$ , Sb  $5s, 5p$ , Ti  $3s, 3p$ , and O  $2s$ . The plane-wave cutoff of 15.1 Ry corresponded to 1000 basis functions per formula unit. For  $\text{Na}_2\text{Sb}_2\text{Ti}_2\text{O}$  we use  $a = 4.144$  Å,  $c = 16.561$  Å, with internal coordinates  $z_{\text{Na}}/c = 0.318$ ,  $z_{\text{Sb}}/c = 0.1212$ .<sup>5</sup> Exchange-correlation energy was included within the local-spin-density approximation (LSDA) as given by von Barth and Hedin.<sup>13</sup> For the Brillouin zone averages, eigenvalues were calculated on a regular mesh of 205 points in the irreducible Brillouin zone and interpolated using the spline Fourier series method.<sup>14</sup>

The Ti ion is of special interest due to the possibility of a  $d^1$  configuration. The  $mmm$  site symmetry of the Ti ion leads to only singly degenerate representations of the  $d$  states, so there are five distinct Ti  $d$  crystal field levels. These can be taken as  $d_{xy}, d_{yz}, d_{zx}$  ( $B_{1u}, B_{2u}, B_{3u}$  symmetry orbitals that are odd under two of the mirror operations) and any two orthogonal linear combinations of  $d_{x^2-y^2}$  and  $d_{3z^2-r^2}$  (both of which are fully symmetric  $A_g$  under  $mmm$ ). If the Sb-Ti-Sb angles were  $90^\circ$  (they are  $88^\circ$  and  $92^\circ$ ), so the Ti sat precisely in the center of a square of Sb ions, the ‘‘local symmetry’’ of Ti would be  $4/m$ . Nearest-neighbor Ti

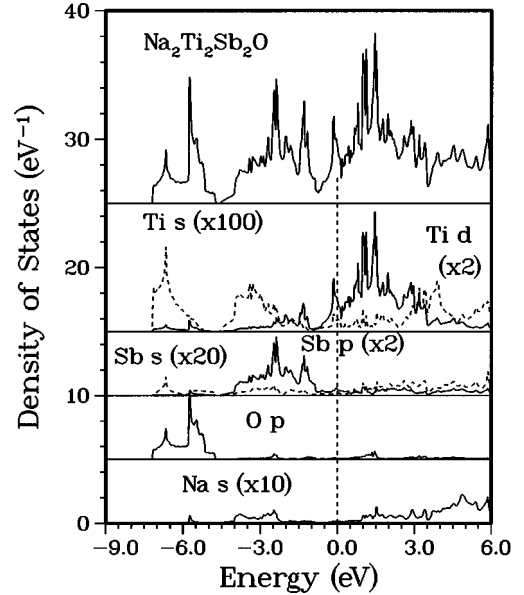


FIG. 2. Total and atom- and orbital-decomposed density of states of paramagnetic  $\text{Na}_2\text{Sb}_2\text{Ti}_2\text{O}$ . The band structure is metallic, with the dotted line denoting the Fermi level. Note the peak in the Ti  $3d$  DOS at the Fermi level.

ions already break this symmetry, however. The O site has  $4/m$  symmetry, while the Na and Sb sites have only  $mm$  symmetry.

## III. INVESTIGATION OF MAGNETIC STATES

Due to the transition seen in the susceptibility and the likelihood of a  $d^1$  configuration on Ti, the possibility of magnetically ordered ground states was studied first.

### A. Paramagnetic case

An initial calculation without spin polarization found the O  $2p$  states to be centered 8 eV below the center of the Ti  $3d$  bands as shown in Fig. 2. This tightly bound behavior is the result of O being surrounded by a charge of  $+14$  ( $4\text{Ti}^{+3} + 2\text{Na}^{+1}$ ). The Sb  $4p$  bands lie between the O  $p$  and Ti  $d$  band complexes and are essentially filled. The relative site energies (more specifically, band centers) relative to the Fermi level ( $E_F$ ) are  $\varepsilon_p^{\text{O}} = -6$  eV,  $\varepsilon_p^{\text{Sb}} = -2.5$  eV,  $\varepsilon_d^{\text{Ti}} = +2$  eV.  $E_F$  falls within bands that are primarily Ti  $3d$ , roughly consistent with an ionic picture with  $\text{Sb}^{-3}$  ions and  $\text{Ti}^{+3}$  ions. The close proximity in energy of Ti and Sb bands ( $\varepsilon_d^{\text{Ti}} - \varepsilon_p^{\text{Sb}} \approx 5$  eV but each is 3–4 eV wide), as well as the tailing of Ti  $d$  DOS into the region of Sb  $p$  DOS and vice versa, indicate dominance of effective  $d$ - $d$  interaction through the Sb states rather than through the O  $p$  states.

For states within a few eV of the Fermi level, the  $\text{Na}^{+1}$  ions appear as spectators only, which is not quite true of the O ions (discussed below). Noting that ionic charges of  $\text{O}^{-2} + 2\text{Na}^{+1}$  cancel, we did a calculation on a fictitious  $\text{Sb}_2\text{Ti}_2$  compound in which Na and O atoms are removed from the cell. Although there are small Madelung shifts, the local densities of states are similar to Fig. 2, reflecting nominally  $\text{Ti}^{+3}$  and  $\text{Sb}^{-3}$  ions. Similarity of the bandwidths to

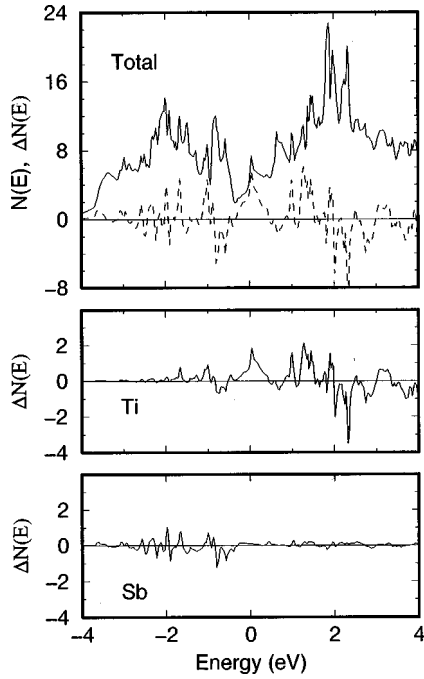


FIG. 3. Total density of states  $N(E)$ , and the spin difference  $\Delta N(E) = N_{\uparrow}(E) - N_{\downarrow}(E)$  (top panel), of ferromagnetic  $\text{Na}_2\text{Sb}_2\text{Ti}_2\text{O}$ , where the moment has been forced to be  $1\mu_B$  per Ti ion, corresponding to  $S = \frac{1}{2}$  ions. Units are states/eV. The difference  $\Delta N(E)$  is decomposed into contributions from Ti  $d$  (middle) and Sb  $p$  (bottom panel) states. As with the paramagnetic case (Fig. 2) the band structure remains metallic. Note the majority peak in the Ti  $3d$  near  $E_F$ ; in spite of this peak, Stoner-like behavior does not stabilize ferromagnetism.

those in the full compound indicate that Ti  $d$ -Sb  $p$  interactions dominate to their respective bandwidths.

In the following subsections we allow various magnetic symmetries, apply external magnetic fields, and investigate the response of the system.

### B. Ferromagnetic order

Given the  $d^1$  configuration of the Ti ion and the (nominally, at least) closed shell nature of the other ions, it is reasonable to expect spontaneous polarization of the ion as commonly occurs in ionic insulators. If the Ti ion is magnetic, there will be a FM state within an energy of order  $J$  per Ti ion of the ground state, where  $J$  is the dominant exchange coupling. To explore magnetic tendencies, FM states with various moments were generated using the fixed-spin-moment method. This method is equivalent to applying a magnetic field to produce a desired net magnetic moment in the unit cell. The energy versus impressed moment, however, is found to be monotonically increasing, following the relation

$$\delta E = \frac{1}{2} \chi^{-1} M^2 \quad (1)$$

up to magnetic moments  $M \leq 0.75\mu_B/\text{Ti}$ . The calculated inverse paramagnetic ‘‘susceptibility’’ was  $\hat{\chi}^{-1} = 1.7 \text{ eV}/\mu_B^2$ . It is clear that there is no FM instability in the system, at least within LSDA.

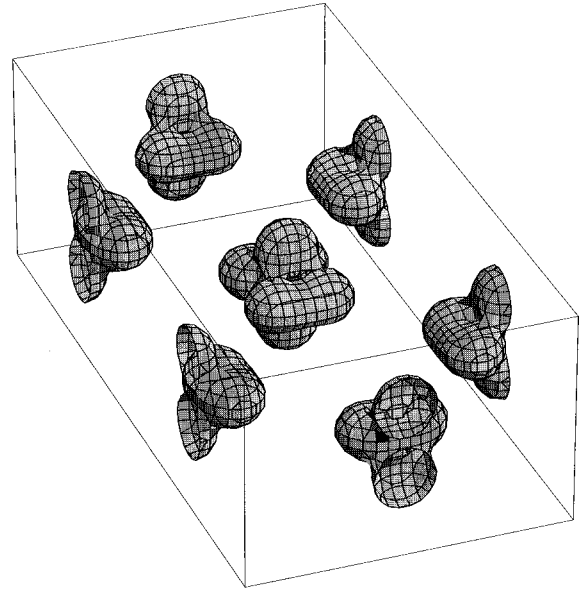


FIG. 4. Isosurface plot of the spin density of the (forced) FM state, shown in the  $\text{Ti}_2\text{O}$  layer containing two primitive cells. The constant density surface at this value of the spin density ( $0.007 \text{ a.u.}$ ) surrounds the Ti ion, and is comprised mostly of  $d_{xy}$  and  $d_{3z^2-r^2}$  character.

In Fig. 3 we show the total (spin-summed) density of states (DOS) for this (forced) FM state, and also the difference  $\Delta N(E) = N_{\uparrow}(E) - N_{\downarrow}(E)$  and its contribution from the Ti  $d$  and Sb  $p$  states. Polarization occurs primarily within the Ti  $d$  bands as expected. The magnetization involves the occupation of a single narrow ( $\leq 0.8 \text{ eV}$ ) majority spin  $d$  DOS peak, and there is a pseudogap separating this band from the unoccupied Ti  $d$  states. The change in the ionic charge arising from the impressed field, as measured by the charge within the spheres around each atom, is negligibly small ( $\leq 0.004$  electrons). The magnetization is roughly 90% on Ti, with 10% on Sb reflecting the hybridization of Ti  $d$  states with Sb  $p$  states. In spite of the pseudogap formation leading to a relatively low value of the Fermi level density of states (DOS)  $N(E_F)$ , this impressed ferromagnetism is highly unstable toward collapse of the Ti moment. We conclude that the electronic structure strongly *disfavors* FM exchange, if in fact the Ti ion is magnetic.

Knowing the character and orientation of the occupied orbital is essential for understanding both the electronic structure and the magnetic interactions. The spin density is shown in Fig. 4. As expected, it lies primarily on the Ti ion, and it is dominated by roughly equal amounts of  $d_{xy}$  and  $d_{3z^2-r^2}$  character. (We take the  $z$  axis to be perpendicular to the  $\text{Ti}_2\text{O}$  layers.)

### C. Antiferromagnetic order AFM1

To explore the simplest antiferromagnetic tendency, we induced an antiferromagnetic state in which the two Ti ions in the cell have oppositely directed spins. The magnetic ions form a simple AFM square lattice, which we denote AFM1, that is vaguely analogous to the AFM state in  $\text{La}_2\text{CuO}_4$ . However, the square Ti lattice is rotated by  $45^\circ$  with respect to the crystal axes, and the Ti spacing is  $a' = a/\sqrt{2}$ . As a

result of this difference, the body-centered stacking of  $\text{Ti}_2\text{O}$  layers leads to Ti ions lying directly above and below other Ti ions and thus does *not* frustrate magnetic order as is the case in  $\text{La}_2\text{CuO}_4$ . Note also that this is a  $\vec{Q}=0$  antiferromagnetism with respect to the crystallographic cell and simply lowers the symmetry from tetragonal to orthorhombic.

A staggered field  $H_{\text{st}}$  was applied, up on one Ti ion and down on the other. Self-consistency of the charge and spin densities was obtained for applied field strengths  $\mu_B H_{\text{st}} \approx 1$  eV. At this point the field is removed. If the AFM state is stable or metastable, the system will relax to a state of this symmetry with nonvanishing spin density. No stable or metastable AFM1 state of this type was found, indicating either that the exchange interactions do not favor this type of ordering or that the Ti ion does not polarize. Considering the crystal structure, which does not suggest strong FM nearest-neighbor coupling, the lack of a spontaneous moment for imposed FM order, and the fact that the observed behavior is nothing like that of the 2D square lattice Heisenberg model, this result is not surprising.

#### D. Antiferromagnetic order AFM2

The Ti-O-Ti superexchange interaction for this geometry will be antiferromagnetic for the  $180^\circ$  bond and (neglecting higher order processes involving polarization of the O ion) zero for the  $90^\circ$  bond. If this exchange coupling were large, it would encourage AFM  $\cdots\text{Ti-O-Ti-O}\cdots$  chains along each of the  $\hat{x}$  and  $\hat{y}$  directions. Considering the tightly bound O  $p$  states, this exchange may be small. If superexchange through the Sb ion is AFM in sign and larger than competing interactions, then one might expect the  $\cdots\text{Ti-Sb}_2\text{-Ti-Sb}_2\cdots$  chains parallel to the planar axes to order antiferromagnetically. Both possibilities lead to AFM order dominated by spin-antialigned Ti-Ti *second* neighbors. This phase, denoted AFM2, has a doubled crystallographic unit cell, for which any nearest-neighbor exchange coupling will be frustrating. Singh, Stryk, and Freitas<sup>15</sup> have considered the consequences if this type of exchange coupling is dominant.

A staggered field was applied as before to induce this type of magnetic order. In Fig. 5 the magnetization versus  $H_{\text{st}}$  is pictured. The Ti moment increases linearly with field until it is fully polarized, then increases more slowly because charge transfer from Sb and O is necessary to increase the moment further. As in the case of AFM1, no spontaneous magnetization is obtained: the moment vanishes when the field is removed. This result implies that AFM next-neighbor coupling does not dominate magnetic interactions sufficiently to produce this ordering, or of course that the Ti ion simply does not polarize.

#### IV. MORE ON THE PARAMAGNETIC PHASE

In these calculations, the local-spin-density approximation has failed to produce a magnetic Ti  $d^1$  ion in any of the ordered FM, AFM1, or AFM2 phases. Experimentally, the character of the ground state is unclear. However, the resistivity shows metallic behavior with  $\rho$  increasing with  $T$ . The magnitude of  $\rho$  is large as measured, but the samples were polycrystalline so the intrinsic value is unknown. The failure

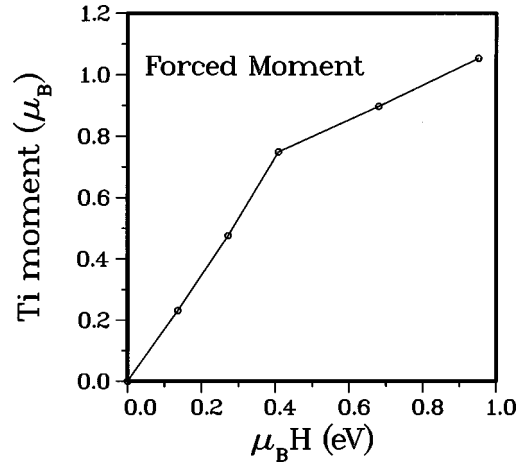


FIG. 5. Calculated moment within a sphere containing most of the Ti spin density—proportional to the Ti moment—versus the applied staggered magnetic field  $H_{\text{st}}$ . The break occurs when the  $d$  orbital is fully polarized (see text).

to obtain any ordered FM, AFM1, or AFM2 state suggests that the Ti ion is not magnetic, so we investigate the paramagnetic LDA predictions in more detail.

#### A. Electronic structure near the Fermi level

The paramagnetic phase is metallic as is evident from Fig. 2, due to overlap of Ti  $d$  bands with Sb  $p$  bands and to a lack of any gap within the Ti  $d$  bands. The band structure along high symmetry directions is presented in Fig. 6. The lowest six bands are primarily Sb  $p$  bands, and the next ten bands (up to about 3 eV about the Fermi energy, taken as zero) are the Ti  $3d$  bands. The Ti  $d$  bands are strongly dispersive, not flat and narrow as would be the case in an ionic insulator. The lowest six valence bands are filled, and there is enough charge (ostensibly the  $d$  electron on each Ti ion) to fill one more band.

Note first that with the ordering of bands shown in Fig. 6 it is impossible to fill a single band, because the next two

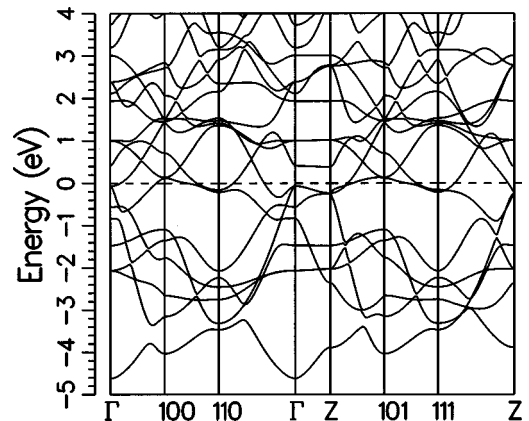


FIG. 6. Band structure of paramagnetic  $\text{Na}_2\text{Sb}_2\text{Ti}_2\text{O}$  along high symmetry directions. The lower six bands comprise the Sb  $p$  band complex. The remaining bands are essentially the Ti  $d$  bands. “101” indicates the point  $(\pi/a, 0, \pi/c^*)$  and similarly for other  $k$  points. (Note that in the body-centered-tetragonal lattice,  $c^* \equiv c/2$  is the height of the primitive cell.)

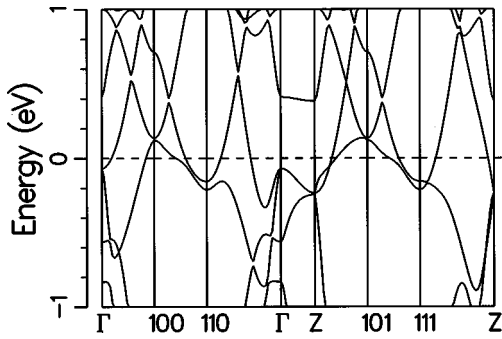


FIG. 7. Enlargement of the bands within 1 eV of the Fermi level.

bands are degenerate along the  $\Gamma$ -Z direction. Thus no simple band shifts can produce an insulating state. For clarity, the band structure near the Fermi level is shown in Fig. 7. Second, there is (as expected) substantial Sb  $p$  character in bands seven and eight; at  $\Gamma$  two purely Ti  $d$  bands sandwich three Sb  $p$  bands in Fig. 7. Less expected is strong O  $p$  character at certain points. At the “110” point in Fig. 7 (the zone corner) the band 1.5 eV above  $E_F$  (hence out of the figure) is 40% O  $p$  with the remainder divided between the two Ti ions. This hybridization is evidence of  $pd\sigma$  interaction, in spite of the O  $p$  band being centered 6 eV below  $E_F$ .

The lowest band with strong Ti  $d$  character (the lower of the two bands crossing  $E_F$ ) is nearly filled, being left with 0.285 holes divided between two  $\hat{c}$ -oriented highly fluted cylinders centered at the (100) and (010) points, as shown in Fig. 8. ( $k$  points will be quoted in units of  $\pi/a, \pi/a, \pi/c^*$ , where  $c^*=c/2$  is the height of the primitive cell.) The next

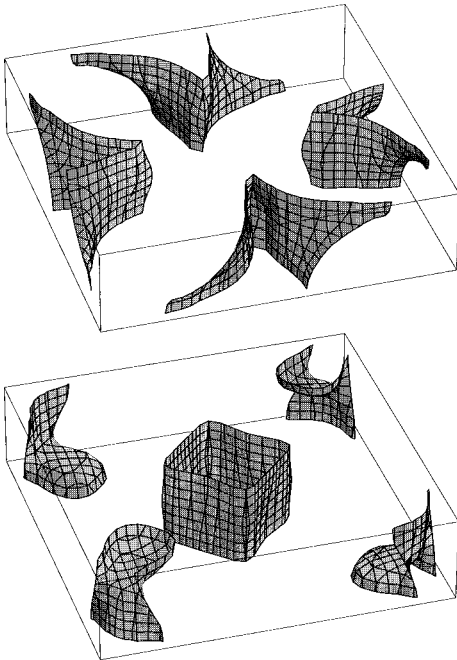


FIG. 8. Fermi surfaces of the lower band (top), comprised of two highly fluted surfaces [at (1,0,0) and (0,1,0)], and the higher band (bottom), a  $\Gamma$  centered fluted surface and the zone corner box Fermi surface. All surfaces are open in the  $k_z$  direction. The  $\Gamma$ -Z line lies along the vertical edges; the zone corner is in the center. Only half of the bct Brillouin zone is shown along the  $z$  direction.

higher band is left with 0.285 electrons, 0.09 of which are in a  $\Gamma$ -Z centered (warped) cylinder. This leaves 0.20 electrons within a very square cylinder (with rounded edges) centered at (1,1,0), also shown in Fig. 8. The 0.20 electron band filling is determined by the relative energies of the two partially occupied bands. This “box” Fermi surface, which has very little dispersion along  $k_z$ , is clearly of very different character from the other two surfaces, which do disperse with  $k_z$ . All Fermi surfaces are open in the  $\hat{c}$  direction, reflecting the layered crystal structure and a very approximate quasi-two-dimensionality.

The dimension of a perfectly square cylindrical box with the same number of electrons is  $\sqrt{(0.10)\pi}/a = 0.32\pi/a$ . Since it is oriented at a  $45^\circ$  angle with respect to the axes, the nesting vector is  $\vec{Q}_F = (0.224, 0.224, 0)\pi/a$ . This strong nesting suggests charge-density wave (CDW) or spin-density wave (SDW) instability with nearly commensurate periodicity

( $\pm \frac{9}{2}a, \pm \frac{9}{2}a$ ) in the  $x$ - $y$  plane. The present work suggests that such a CDW (or SDW) could account for the drop in the susceptibility and increase in the resistivity at  $T^*$  by gapping the box Fermi surface. The box contains 27% of the Fermi level density of states,  $N(E_F) = 4.77$  states/eV. However, if this Fermi surface is strongly enhanced by nested scattering processes, gapping of the box could lead to much more than a 27% drop in the susceptibility at the CDW/SDW transition.

The box Fermi surface is almost completely Ti  $d_{xy}$  in character. The in-plane character of  $d_{xy}$  immediately accounts for the lack of  $k_z$  dispersion. That direct Ti-Ti overlap is important is not surprising, since the distance ( $a' = a/\sqrt{2} = 2.94$  Å) is the same as in Ti metal. By themselves, the  $dd\sigma$  overlap between neighboring Ti ions (two per primitive cell) would lead to two bands, one of which would disperse only along the (1,1,0) direction and the other only along (1,-1,0). In the region of  $(\pi/a, \pi/a, 0)$  the Sb  $p$ -derived bands lie considerably lower, so this simple, pure Ti  $d_{xy}$  character dominates near (1,1,0). This behavior persists only a certain distance from the (1,1,0) point, which includes the position of the box Fermi surface. Beyond that point, these bands mix with Sb  $p$  bands and the other, more complicated, Fermi surfaces result.

The fact that the box surface is Ti-dominated suggests consideration of the Ti sublattice, which by itself forms a square lattice of dimension  $a'$  oriented at  $45^\circ$  with respect to the crystal axes. In the corresponding doubled and rotated Brillouin zone the box surface appears at the  $X' = (\pi/a', 0, 0)$  point.

To illustrate the full behavior of band 8, in Fig. 9 we show a top view of the constant energy surfaces starting at  $E_F - 0.1$  eV and successively increasing by 0.1 eV. The nearly dispersionless (along  $k_z$ ) behavior, which shows up as slightly thickened lines, persists to 0.4 eV above  $E_F$ , where the band mixes with bands with more Sb, and some O, character. Some circular constant energy surfaces also appear around the  $X$  point somewhat above  $E_F$ .

In spite of the low dimensionality of the box Fermi surface, the overall behavior of the carriers is three dimensional. The rms Fermi velocities are  $v_x = v_y = 1.6 \times 10^7$  cm/s,  $v_z = 0.95 \times 10^7$  cm/s, an anisotropy of less than a factor of 2. The Drude plasma energies, which are important in analysis

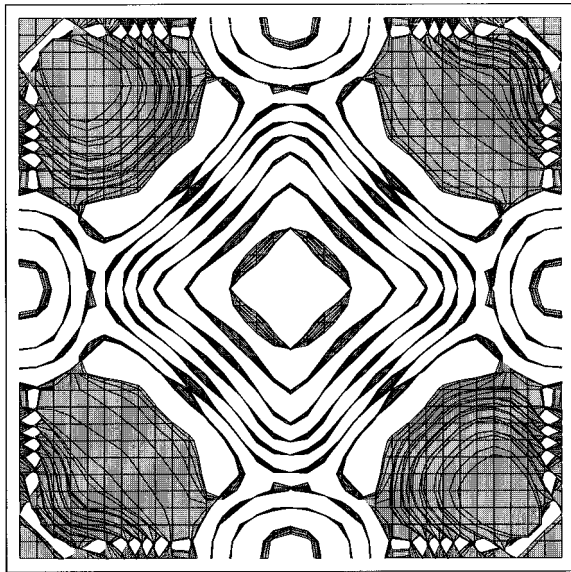


FIG. 9. Projection onto the  $k_z=0$  plane of constant energy surfaces of band 8 at  $-0.1, 0.0, 0.1,$  and  $0.2$  eV relative to the Fermi level, illustrating the evolution of the band giving rise to the box Fermi surface. White space indicates no projected states. The second-innermost constant energy surface (i.e., near the center of the plot) is the box Fermi surface.

of transport data, are  $\hbar\Omega_{p,xx}=\hbar\Omega_{p,yy}=3.0$  eV,  $\hbar\Omega_{p,zz}=1.7$  eV, which are not uncommon values for transition-metal compounds.

## V. SUMMARY

The tendency towards magnetic order and the general electronic structure of  $\text{Na}_2\text{Sb}_2\text{Ti}_2\text{O}$  have been studied within

the local-density approximation. No inclination of the Ti ion to become magnetic was found, so the transition observed in the temperature dependence of the susceptibility cannot be ascribed to ordering of a magnetic Ti  $d^1$  ion.

A square Fermi surface, nearly dispersionless in the  $k_z$  direction, suggests a CDW or SDW that gaps this surface as the underlying cause of the transition. Without knowledge of the relative strengths of the electronic and magnetic matrix elements, it is not possible to pinpoint one or the other. The box Fermi surface is very strongly Ti  $d$  in character, so the resulting CDW or SDW will involve primarily the Ti ion. The extremely flat Fermi surfaces suggest the possibility of non-Fermi-liquid behavior, although an important distinction between this compound and the strongly nested Fermi liquids that have been studied recently is that in this compound there are additional non-nested scattering processes for the carriers to participate in.

The inverse- $\text{K}_2\text{NiO}_4$  structure seemed to invite analogy with  $\text{La}_2\text{CuO}_4$ . This work has shown that there is very little analogy. The electronic structure is much more three dimensional, and the transition-metal ions seem to be unpolarized. Establishing the importance of direct Ti-Ti coupling is perhaps the most important result of this paper, and it is this coupling that leads to the potentially very important box Fermi surface.

## ACKNOWLEDGMENTS

I acknowledge stimulating discussions with S.M. Kauzlarich, R.R.P. Singh, and D. Khomskii. I appreciate communication by S.M.K. and R.R.P.S. of their results prior to publication. This work was supported by the Office of Naval Research. Computation was done at the Arctic Region Supercomputing Center.

<sup>1</sup>E. Dagotto and T. M. Rice, *Science* **271**, 618 (1996).

<sup>2</sup>M. O'Keefe and F. S. Stone, *J. Phys. Chem. Solids* **23**, 261 (1962).

<sup>3</sup>P. W. Anderson, *Mater. Res. Bull.* **8**, 153 (1973).

<sup>4</sup>K. Takeda, K. Miyake, T. Takeda, and K. Hirakawa, *J. Phys. Soc. Jpn.* **61**, 2156 (1992).

<sup>5</sup>A. Adam and H.-U. Schuster, *Z. Anorg. Allg. Chem.* **584**, 150 (1990).

<sup>6</sup>E. A. Axtell III, T. Ozawa, S. M. Kauzlarich, and R. R. P. Singh, *J. Solid State Chem.* **134**, 423 (1998).

<sup>7</sup>W. Geertsma and D. Khomskii, *Phys. Rev. B* **54**, 3011 (1996).

<sup>8</sup>J. B. Goodenough, *Magnetism and the Chemical Bond* (Wiley, New York, 1963), Chap. IIIC.

<sup>9</sup>W. E. Pickett, *Phys. Rev. Lett.* **79**, 1746 (1997).

<sup>10</sup>W. E. Pickett, *Rev. Mod. Phys.* **61**, 433 (1989).

<sup>11</sup>S. H. Wei and H. Krakauer, *Phys. Rev. Lett.* **55**, 1200 (1985); D. J. Singh, *Phys. Rev. B* **43**, 6388 (1991).

<sup>12</sup>D. J. Singh, *Planewaves, Pseudopotentials, and the LAPW Method* (Kluwer Academic, Boston, 1994).

<sup>13</sup>U. von Barth and L. Hedin, *J. Phys. C* **5**, 1629 (1972).

<sup>14</sup>W. E. Pickett, H. Krakauer, and P. B. Allen, *Phys. Rev. B* **38**, 2721 (1988).

<sup>15</sup>R. R. P. Singh, O. A. Staryk, and P. J. Freitas, *J. Appl. Phys.* **83**, 7387 (1998).